INTERNATIONAL JOURNAL OF SCIENCE AND NATURE

www.scienceandnature.org

SCHIFF BASE DERIVED FROM 5-BROMO-ISATIN AS CARBON STEEL CORROSION INHIBITOR IN 3.5% NaCl: EXPERIMENTAL AND THEORETICAL EVALUATION

Rehab Majed Kubba & Dhuha Abdul-Kareem Challoob
Department of Chemistry, College of Science, University of Baghdad, Baghdad, Iraq.

ABSTRACT
The inhibition activity of a new Schiff base derived from 5-Bromo-isatin namely N-[(6-nitro-1, 2- dihydrophtalazin -3,10-dione-1-yl) aceto] 3(tolylimino)-5-bromo-2-oxoindole (5BIN), for carbon steel in aerated 3.5% NaCl solution was investigated using open circuit potential (OCP), potentiodynamic to evaluate the 5BIN inhibition efficiency. Results from potentiodynamic polarization revealed the mode of inhibitive action and adsorption of inhibitor molecules. Further, surface morphological was examined by SEM (Scanning Electron Microscopy), AFM (Atomic Force Microscopy), and EDS (Energy Dispersive Spectroscopy) measurements, all supported the protective film formation by 5BIN on carbon steel surface. Quantum mechanical methods of the approximate semiempirical theory PM3 and DFT (Density Functional Theory) of B3LYP with a level of 6-311++G (2d, 2p) were used for calculating the geometrical structure, physical properties and inhibition efficiency parameters, all were studied at the equilibrium geometry in three media (vacuum, DMSO, and H_2O). The theoretical results corroborated by experimental data, with both the experimental and theoretical data showing that the 5BIN is a very good corrosion inhibitor.

KEYWORDS: Corrosion inhibitor, 3.5% NaCl solution, 5-Bromo-isatin derivative.

INTRODUCTION

The use of inhibitors is one of the most practical ways to protect steel against corrosion in salt solutions[1]. The majority of inhibitors used in the industry are organic compounds. It is mainly composed of nitrogen, oxygen and sulfur, as well as double or triple bonds that facilitate the absorption of these compounds to metal surfaces[2]. The mechanism of inhibition is predominantly occur by some physicochemical and electronic properties of organic inhibitor that relate to functional groups, exceptional effects, electron density of donor atoms, and orbital nature of electrons donation[3,4]. Isatin is one of a new class of compounds, not homogeneous with significant and well tolerated in humans, and can give different activities by entering substations into its loop. This can increase its adsorption capacity and make it a good inhibitor[5,6]. The Sanimir method[7,8] was the oldest and most important methods in the preparation of the isatin, but this method was limited by Ganeshwara[9]. For ethane derivatives, nitrogen arsenic derivatives can be prepared using a mixture of sulfonitric 5 nitrozatin[10]. Preparation of bromine arsenic derivatives achieved in two methods, the first in alcohol gives 5,7-Dibromo-3,3-dialkoxyoxindoles in an acid catalyzed ketalization of the halogenated isatin [11], and the second is monobromoisatin production in position 5 (at least on a micorscale) by the use of N-bromoacetamide in acetic acid medium [12]. Isatin and isatin derivative have more applications like antibacterial, anti-HIV, antifungal, anti-cancer, anticonvulsant, anti-inflammatory, and anti-depressant[13,14].Quantum mechanical methods and molecular modeling techniques enable the definition of a large number of molecular quantities characterizing, shape, the reactivity, and binding properties as well as molecular fragments and substituent. The use of theoretical parameters presents two main advantages: firstly, the compound and their various fragments and substituent can be directly characterized on the basis of their molecular structure; and secondly, the proposed mechanism of action can be directly accounted in terms of the chemical reactivity of the compounds under study. The inhibiting efficiency of the corrosion inhibitor depends on the number of adsorption actives center in the molecule, the charge density, size, aromaticity, sterric factor, electron density at donor molecule, the electronic structure of inhibiting molecules, formation of the metallic complex, and mode of adsorption [15,16].

The aim of this work is to synthesize and characterize a new derivative of 5-bromo isatin which is N-[(6-nitro-1, 2-dihydrophtalazin-3,10-dione-1-yl) aceto] 3 (tolylimino)-5-bromo-2-oxoindole (5BIN), Figure 1. Then the viability study of the corrosion inhibition theoretically and experimentally for carbon steel C45 surface in three media (vacuum, dimethyl sulphoxide, and water), which was tested first theoretically among many newly derivatives of the 5-bromo isatin [17] as a best one for being corrosion inhibitor, depending on studying the parameters of quantum mechanical inhibition efficiency using PM3 and DFT quantum mechanical methods. Practically to proven that, 5BIN could be used as a corrosion inhibitor for the surface of carbon steel in 3.5% NaCl solution, a measurements of linear polarization resistance, SEM (Scanning Electron Microscopy), AFM (Atomic Force Microscopy) and EDS (Energy Dispersive Spectroscopy) were used.

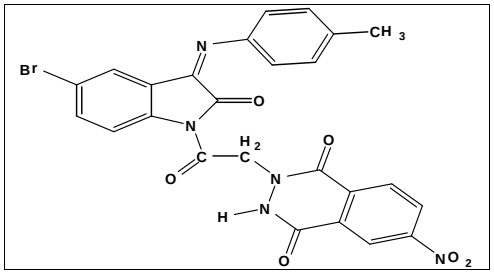

FIGURE 1: Chemical structure of N-[(6-nitro-1,2-dihydrophtalazin-3,10-dione-1-yl) aceto] 3(tolylimino)-5-bromo-2-oxoindole (5BIN).

Theoretical calculations

Complete geometrical optimization of the investigated molecule are performed using semiemperical method PM3 and DFT (Density Functional Theory) using Becke′s three-parameter functional and the correlation functional of Lee, Yang and Parr (B3LYP) with a 6-311++G (2d, 2p) level of theory [18-20], implemented in Gaussian 09 program package [21]. The theoretical parameters that were calculated at the optimized structure are E_{HOMO} (Energy of the Highest Occupied Molecular Orbital), E_{LUMO} (Energy of the Lowest Unoccupied Molecular Orbital), $\Delta E_{HOMO-LUMO}$ (Energy gap), dipole moment (μ), electron affinity (A), ionization potential (I) and the fraction of electrons transferred (ΔN)……*etc*..

MATERIALS & METHODS

Synthesis of 3-(tolyl-imino)-5-bromo indole-1H-2 one (1)

A mixture of 5-bromo-isatin (Indole-2, 3-Dione) (4.20, 0.0186 moL) with p-toluidine (5.87, 0.0186 moL) in dimethylformamide (10 mL) was refluxed for (10 hrs) in the presence of (4-5) drops of glacial acetic acid. After cooling, it was filtered and recrystallized from dioxan solvent [22].

Synthesis of N-(α-chloroaceto-1-yl)-3-(P-tolyl imino)-5-bromo-2-oxo- indole (2)

A mixture of (1g, 0.0031moL) compound (1) in (5 mL) dimethylformamide (DMF) was cold to (0 ^{o}C). A solution of sodium hydride (0.08 g, 0.0031 mol 60% in mineral oil) was periodically added to the mixture in a small portions. Chloroacetyl chloride (0.24 mL, 0.0031 moL) was added to the slurry via stirring, and the reaction mixture was slowly warmed to room temperature. The reaction was quenched with water after (4.5 hrs). The resulting precipitate was removed via filtration and recrystallization from ethanol solvent [22].

Synthesis of N-(acetohydrazide-1-yl)-3-(*P*-tolyl imino)-5-bromo-2-oxo-indole (3).

To a mixture of compound (2), (1 g, 0.0025 mol.) in absolute ethanol (5 mL) with drops of dimethylformamide, hydrazine hydrated 80% (0.07 mL, 0.0025 mol) was added with continuous stirring. The resulting mixture was refluxed for (4 hrs). After cooling by adding to ice water, a deep brown precipitate was formed. The precipitate was filtered and recrystallized from ethanol solvent [23].

Synthesis of N-[(6-nitro- 1, 2- dihydrophtalazin-3, 10-dione-1-yl) aceto] 3(tolylimino) -5-bromo-2-oxoindole (4)

A mixture of (1g, 0.0025moL) compound (3) with (4-nitrophthalic anhydride) (0.0025moL) in (10mL) glacial acetic acid was heated under reflux for (6-8hrs). The mixture was cooled by adding to ice water. After cooling, a deep yellow precipitate was formed. The precipitate was filtered and recrystallized from chloroform solvent [24].

Preparation samples

In this study a carbon steel (C45) was used with a chemical composition of metallic materials (in wt%) of (0.42-0.50)% C, 0.40% Si, (0.50-0.80) % Mn, 0.045% S, 0.40% Cr, 0.045% P, 0.40% Ni, 0.1% (Mo & Cr) and (97.31-97.96)% is iron (Fe). The carbon steel samples were mechanically cut into the circular sample with dimension of 2.5cm in diameter and 0.5 mm thickness. Pre-treated prior to the experiments by grinding with emery paper SiC in different grade (80, 150, 220, 320, 400, 1000, 1200 and 2000), rinsed with tap water, de-ionized water and recent degreased in acetone, washed again with de-ionized water, dried at room temperature and kept in a desiccators before immersed in the corrosive solution [25,26].

Preparation solutions

Blank solution

35gm of NaCl was dissolved in (100mL) de-ionized water, transferred quantitatively to (1000mL) volumetric flask, adding (2ml of DMSO) then complete the volume to one liter with de-ionized water. In this study, 3.5% NaCl was choosen to avoid the problems linked to the ohmic drop [27].

5BIN solutions

The solutions concentration of (5ppm, 10ppm, 20ppm, and 30ppm) were prepared by dissolving 0.005g, 0.01g, 0.02g, and 0.03g of 5BIN respectively, each in 2mL DMSO, transferred to a volumetric flask of 1L containing 35g NaCl dissolved in de-ionized water. The volume was completed to 1L with de-ionized water.

Electrochemical measurements

The potentiostat set up includes host computer, thermostat, magnetic stirrer, Matlab (Germany, 2000) potentiostat, and galvanostat. The corrosion cell is (1L) capacity made of pyrex, consists of two bowls internal and external. The corrosion cell is a three electrode electrochemical cell containing a carbon steel working electrode with a 1 cm^2 surface are used to determine the potential of working electrode according to the reference electrode, a platinum auxiliary electrode with length of 10 cm and a silver-silver chloride (Ag/AgCl, 3.0M KCl) referenced electrode. The working electrode was immersed in the test solution for 15 minute to establish steady state open circuit potential (Eocp), then electrochemical measurements were performed in potential range (±200) mV. All

electrochemical tests have been performed in aerated solutions at 293, 303, 313, 323, and 333 K.

RESULTS & DISCUSSION

Molecular geometry

The 5BIN compound was built using Gaussian 09 package for calculating the equilibrium geometries[21]. The corresponding geometry in vacuum was fully optimized using PM3, and DFT methods. The geometry of the investigated molecule was calculated in addition to vacuum, by two solution media (H_2O and DMSO) at the same level of DFT theory. The final geometry of (5BIN) according to the most correct method DFT is given in Figure 2b.

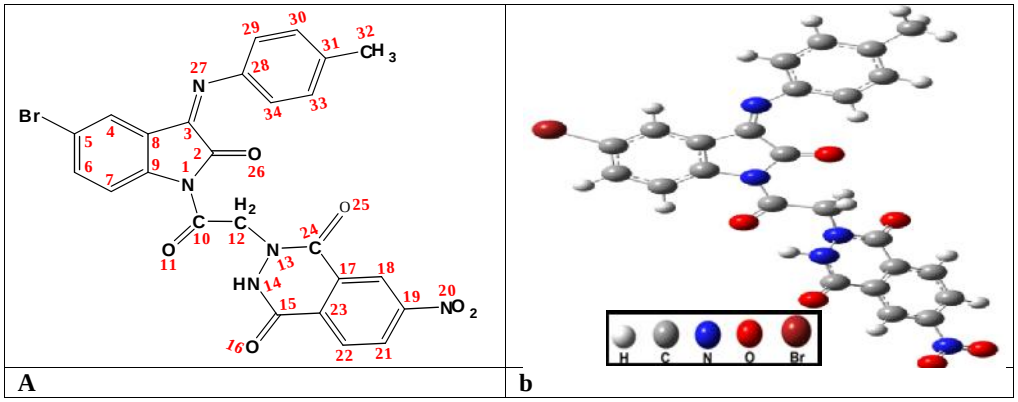

FIGURE 2: a- Chemical structure of 5BIN**, b-** Equilibrium geometry of the 5BIN molecule calculated by DFT method**.**

Figure 2a shows the label of atoms for 5BIN inhibitor. The different substitutions at N27 and C12 made a difference observed in the computational results involves significant modifications on the geometrical structure Table 1, physical properties Tables (2,4) inhibition efficiency parameters Tables (3,5) in compares with other 5-Bromo isatin derivitives studied previously[28-30]. The optimized geometrical structure of 5BIN compound was found to be the same in the three media. The longest bond length was observed for C5-Br (1.917A^0), then the bond length of C10-C12 (1.522A^0). The shortest bond length was observed for C32-H (1.089A0). The bond angles for the compound getting between (104.963A^0) in C2C3C8 and (134.473A^0) in C3N27C28**.** The values of trans dihedral angles such as (N27C28C29C30), (C28C29C30H), (N27C28C34C33), (C18C17C23C24), and cis dihedral angles such as (HC29C30H), (N20C19C21H), (BrC5C6H35), (C18C19 C21C22) shown that 5BIN molecule is nearly planar. This result leads to explain that the adsorption on the metallic surface was easier through these sites of 5BIN, Table 1. On using the solvents, no changes were observed in the geometrical structure.

TABLE 1: DFT geometrical structure calculation for (5BIN) molecule

Description Bond length	Bond length (Å)	Description angle (deg)	Bond angle (deg)	Description Dihedral angle	Dihedral angle (deg)
N1-C2	1.426G	N1C2C3	106.444G	BrC5C6H35	-0.055G
N1-C9	1.431G	N1C2O26	123.889G	C4C5C6C7	0.101G
N1-C10	1.396G	C2C3C8	104.963G	C5C6C7C9	0.117G
C2-C3	1.519G	C3C8C9	109.972G	C5C4C8C9	-0.064G
C2=O26	1.207G	C8C3N27	121.725G	C8C9N1C2	1.388G
C3-C8	1.462G	N1C9C8	108.866G	O26C2N1C10	2.981G
C3-N27	1.281G	C9C8C4	121.057G	C9N1C10O11	-4.587G
C4-C5	1.388G	C8C4C5	117.658G	C10C12N13N14	-63.002G
C4-C8	1.387G	C4C5Br	119.243G	HN14C15O16	-27.581G
C5-C6	1.390G	C4C5C6	121.601G	C15N14N13C24	-22.713G
C5-Br	1.917G	C5C6C7	120.727G	C15C17C23C24	1.367G
C6-C7	1.394G	C6C7C9	117.848G	C18C17C23C22	-0.674G
C7-C9	1.387G	C7C8C9	121.105G	C15C17C18H	-0.892G
C9-C8	1.398G	N1C10O11	120.370G	C18C19C21C22	-0.050G
C10-C12	1.522G	N1C10C12	118.264G	C19C21C22C23	-0.076G
C12-N13	1.461G	C10C12N13	111.545G	HC21C22H	-0.129G
N13-N14	1.418G	C12N13N14	114.124G	N20C19C21H	0.043G
N14-C15	1.376G	N13N14C15	122.862G	C18C19N20O35	-6.824G
C15=O16	1.220G	N14C15O16	120.572G	N27C28C29H	0.218G
C15-C17	1.481G	N14C15C17	115.411G	HC29C30H	0.046G
C17-C18	1.390G	C17C15O16	123.988G	C28C29C30C31	0.064G
C18-C19	1.386G	C15C17C23	120.329G	C5C4C8C3	178.957G
C19-N20	1.478G	C17C23C24	121.178G	C6C7C9N1	-178.242G
N20-O35	1.223G	C23C24N13	121.178G	C2C3C8C4	-179.499G
N20-O36	1.224G	C23C24O25	122.477G	C8C3C2O26	-177.610G
C19-C21	1.394G	C23C22C21	119.981G	N27C28C29C30	-179.926G

C21-C22	1.387G	C19C21C22	118.684G	C3N27C28C29	179.322G
C22-C23	1.394G	C21C19N20	118.772G	C28C29C30H	-179.804G
C23-C17	1.398G	C19N20O35	117.409G	N27C28C34C33	179.944G
C23-C24	1.487G	C19N20O36	117.282G	C24N13N14H	-161.094G
C24=O25	1.223G	C21C22C23	119.981G	N14N13C24O25	-166.801G
C24-N13	1.380G	C22C23C17	120.251G	C12N13C24C23	164.177G
N27-C28	1.385G	C18C19C21	122.447G	C22C23C24N13	175.979G
C28-C29	1.408G	C3N27C28	134.473G	C17C23C22H	-179.658G
C10=O11	1.216G	N27C28C29	113.707G	C23C17C15O16	174.267G
C29-C30	1.388G	C29C28C34	118.193G	C21C19C18H	179.859G
C30-C31	1.396G	C28C29C30	121.181G	C21C19N20O35	173.226G
C31-C32	1.504G	C29C30C31	120.577G	C17C19N20O36	-175.013G
C32-H	1.089G	C30C32C33	118.374G	C18C17C23C24	179.960G
C31-C33	1.397G	C30C31C32	120.798G	C15C17C23C22	-179.267G
C33-C34	1.390G	C31C32H	111.383G	C21C22C23C24	179.817G
C34-C28	1.408G	C31C33C34	121.744G	C15C17C18C19	179.146G

Reactivity sites

Limits orbital theory is useful in predicting absorption inhibitor molecules responsible centers to interact with the metal [31]. Conditions that involve molecular orbital border can provide the authoritarian contribution, due to the inverse of the energy dependence of the stability of the orbital energy difference ($\Delta E = E_{LUMO}-E_{HOMO}$). These orbitals, also called Frontier orbitals, determine the way the molecule interacts with other species. The HOMO is the orbital that could act as an electron donor, since it is the outermost (highest energy) orbital containing electrons. The LUMO is the orbital that could act as the electron acceptor, since it is the innermost (lowest energy) orbital that has room to accept electrons. According to the frontier molecular orbital theory, the formation of a transition state is due to an interaction between the Frontier orbitals (HOMO and LUMO) of reactants. The energy of the HOMO is directly related to the ionization potential, and the energy of the LUMO is directly related to the electron affinity. The $\Delta E_{HOMO-LUMO}$ gap, i.e. the difference in energy between the HOMO and LUMO, is an important stability index. A large $\Delta E_{HOMO-LUMO}$ gap implies high stability for the molecule in chemical reactions. The concept of ''activation hardness" has been also defined on the basis of the $\Delta E_{HOMO-LUMO}$ energy gap. The qualitative definition of hardness is closely related to the polarizability, since a decrease of the energy gap usually leads to easier polarization of the molecule. Quantum chemical parameters expense related to the efficiency of the inhibition of a molecule, such as HOMO and LUMO energy values, frontier orbital energy gap, molecular dipole moment, electronegativity (χ), global hardness (η), softness (σ), the fraction of electron transferred (ΔN), were calculated using the DFT method and have been used to understand the properties and activity of the newly prepared compound and to help in the explanation of the experimental data obtained for the corrosion process. According to Koopman's theorem [32], the ionization potential (IE) and electron affinity (EA) of the inhibitors are calculated using the following Equations:

$IE = -E_{HOMO}$ (1)

$EA = -E_{LUMO}$ (2)

Thus, the values of the electronegativity (χ) and the chemical hardness (η) according to Pearson, operational and approximate definitions can be evaluated using the following relations [33].

$$\chi = (IE+EA)/2 \quad (3)$$

$$\eta = (IE-EA)/2 \quad (4)$$

Global chemical softness (S), which describes the capacity of an atom or group of atoms to receive electrons [34], was estimated by using Equation 5:

$$S = 1/\eta \quad (5)$$

The number of transferred electrons (ΔN) was also calculated depending on the quantum chemical method [35, 36], by according to Equation 6:

$$\Delta N = (\chi_{Fe}-\chi_{inhib.})/[2(\eta_{Fe} + \eta_{inhib.})] \quad (6)$$

Using a theoretical values for mild steel $i_{Fe=}$ 7.0 eV. mol^{-1} and η_{Fe} = 0.0eV. mol^{-1} [37]. χ_{Fe} denote the absolute electronegativity of iron and i_{inh} the electronegativity of inhibitor molecule. η_{Fe} and η_{inh} denote the absolute hardness of iron and the inhibitor molecule respectively. The dipole moment (μ in Debye) is another very important electronic parameter, its product from uniform distribution charge on the atoms and the distance between the two bonded atoms [38]. High dipole moment values are reported to facilitate adsorption and therefore inhibition by influencing the transport process through the adsorbed layer[39,40]. At vacuum medium the dipole moment values of 5BIN are (7.16827 Debye) for PM3 and (9.0893 Debye) for DFT, increased in solutions of DMSO and H_2O Tables 2, 4. Probably indicating a strong dipole-dipole interactions and the adsorption of 5-bromoisatin derivative in aqueous solution can be regarded as a quasi-substitution process of the DMSO and water molecules by the inhibitor molecules at the metal surface (DMSOads and H_2Oads).

TABLE 2: PM3 calculations for some physical properties of the inhibitor molecule 5BIN at the equilibrium geometry

M. formula M. wt. (gm/mol)	ΔH^0_f (kcal/mol) (kJ/mol)	E_{HOMO} (eV)	E_{LUMO} (eV)	$\Delta E_{HOMO-LUMO}$ (eV)	μ (Debye)
$C_{25}H_{16}N_5O_6Br$ 562.335	-14.014 -58.637	-9.330	-1.982	7.348	7.16827

TABLE 3: Quantum chemical parameters for the inhibitor molecules 5BIN as calculated using PM3 method

IE eV)	EA (eV)	η (eV)	χ (eV)	S (eV)	(eV)	ΔN
9.330	1.982	3.6740	5.6560	0.2721	4.3536	0.1829

TABLE 4: DFT calculations for some physical properties of the 5BIN inhibitor in three media (vacuum, DMSO, and H_2O) at the equilibrium geometry

Inhib. medium	Sym	E_{HOMO} (eV)	E_{LUMO} (eV)	$\Delta E_{HOMO-LUMO}$ (eV)	μ (Debye)	E_{total} (eV)
Vacuum	C1	-6.8031	-3.5853	3.2178	9.0893	-103187.8972
DMSO	C1	-6.5457	-3.4683	3.0774	10.2178	-115974.3663
H_2O	C1	-6.5435	-3.4689	3.0746	10.2282	-115974.3772

TABLE 5: Quantum chemical parameters for the 5BIN inhibitor in three media (vacuum, DMSO, and H_2O) as calculated using DFT method

Inhib. Medium	IE (eV)	EA (eV)	η (eV)	χ (eV)	S (eV)	(eV)	ΔN
Vacuum	6.8031	3.5853	1.6089	5.1942	0.6215	8.3845	0.5611
DMSO	6.5457	3.4683	1.5387	5.007	0.6498	8.1465	0.6476
H_2O	6.5435	3.4689	1.5373	5.0062	0.6504	8.1513	0.6484

The Frontier molecule orbital density distributions of 5BIN as calculations using DFT method is shown in Figure 3.

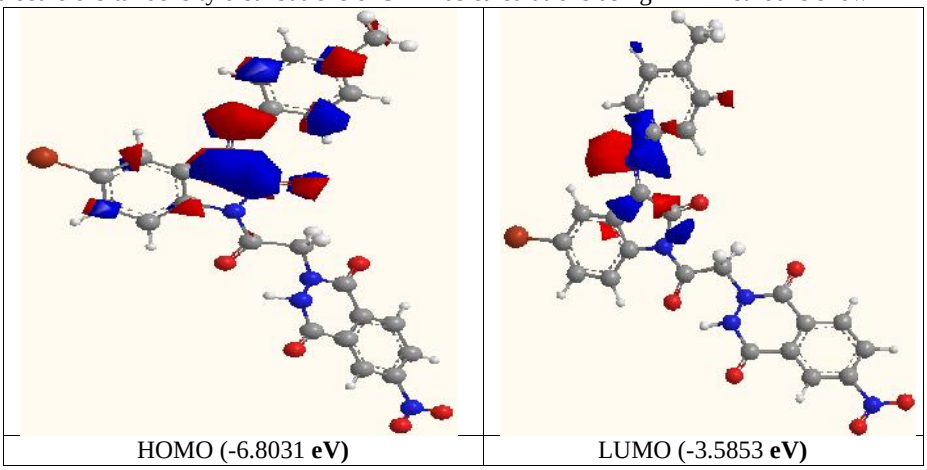

HOMO (-6.8031 **eV)** LUMO (-3.5853 **eV)**

FIGURE 3: DFT calculations for Frontier molecule orbital density distributions of 5BIN. Red color: negative charged lobe, blue color: positive charge lobe.

Local reactivity of the one N-benzyl-5-bromo isatin derivative

The local reactivity sites of the studied inhibitors are investigated using the DFT Mulliken charges population analysis which is an indication of the reactive sites of molecules (nucleophilic and electrophilic sites). Therefore, the molecule regions where the electronic charge is large are chemically softer than the regions where the electronic charge is small. So the electron density plays an important role in calculating the chemical reactivity. Chemical adsorption interactions are either by electrostatic or orbital interactions. Electrical charges in the molecule considered driving force of electrostatic interactions, so they are important in physico chemical properties of compound reactions[41,42]. The sites for electrophihic attack were controlled by the positive charges, in turn; the site for electrophilic attack was controlled by the negative charges. From Table 6, the order of the negative active sites for adsorption (nucleophihic reactive sites) is: O16> O25> C18> O11> C12> O26> N14> C30 and the order of positive active sites for adsorption (electrophihic reactive sites) are C24> C10> C15.

TABLE 6: DFT Mulliken charges population analysis for the 5BIN molecule in the three media (vacuum, DMSO, and H_2O).

Atom	Electronic charge (ecu)	**Atom**	Electronic charge (ecu)	**Atom**	Electronic charge (ecu)	**Atom**	Electronic charge (ecu)
N1	-0.161V	C9	0.221V	C18	-0.511V	C28	0.088V
	-0.127D		0.223D		-0.461D		0.105D
	-0.126W		0.223W		-0.460W		0.106W
C2	0.331V	C10	0.496V	C19	-0.056V	C29	-0.096V
	0.352D		0.564D		-0.157D		-0.108D
	0.352W		0.565W		-0.159W		-0.108W
C3	-0.055V	O11	-0.439V	N20	0.016V	C30	-0.368V
	-0.026D		-0.469D		0.081D		-0.402D
	-0.025W		-0.470W		0.082W		-0.402W
C4	-0.308V	C12	-0.403V	C21	-0.042V	C31	0.388V
	-0.275D		-0.438D		-0.035D		0.372D
	-0.274W		-0.439W		-0.035W		0.371W
C5	-0.158V	N13	0.242V	C22	-0.349V	C32	-0.319V
	-0.192D		0.251D		-0.353D		-0.332D
	-0.192W		0.251W		-0.353W		-0.332W
Br	-0.051V	N14	-0.411V	C24	0.630V	C33	-0.158V
	-0.063D		-0.390D		0.663D		-0.169D
	-0.063W		-0.389W		0.664W		-0.169W
C6	-0.303V	C15	0.373V	O25	-0.486V	C34	-0.168V
	-0.301D		0.402D		-0.551D		-0.175D
	-0.302W		0.403W		-0.552W		-0.175W
C7	-0.153V	O16	-0.475V	O26	-0.389V	O35	-0.122V
	-0.170D		-0.555D		-0.419D		-0.175D
	-0.170W		-0.556W		-0.419W		-0.176W
C8	0.321V	C17	0.313V	N27	-0.215V	O36	-0.134V
	0.302D		0.384D		-0.251D		-0.177D
	0.302W		0.386W		-0.252W		-0.178W

V: vacuum, D: DMSO, W: water, blue color: positive charge (electrophihic active sites), red color: negative charge (nucleophihic active sites).

Synthesis of of 3-(tolyl-imino) -5-bromo indole-1H-2-one (1)

A mixture of 5-bromoisatin (indole-2,3-dione) and para methyl aromatic amine in dimethylformamide was refluxed. in presence of glacial acetic acid to give compound (1), Scheme 1.

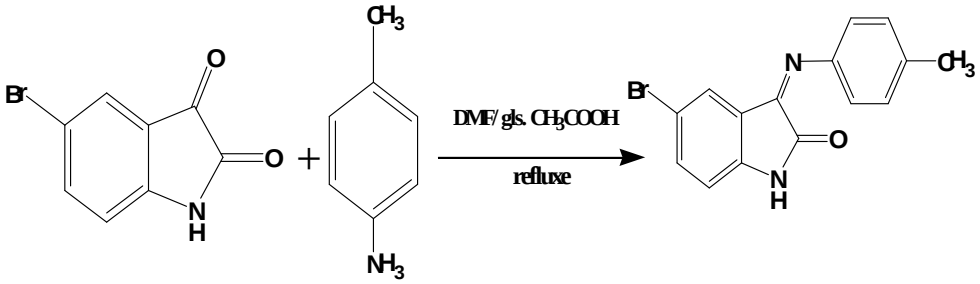

Scheme 1: Synthesis of 3-(tolyl-imino)-5-bromo indole-1H-2-one.

The first step is the condensation reaction between para methyl aromatic amine and carbonyl compounds involved nucleophilic addition of para methyl aromatic amine compound to a carbonyl group producing intermediate which eliminate water molecule in step two [43] to afford the compound (1), Scheme 2.

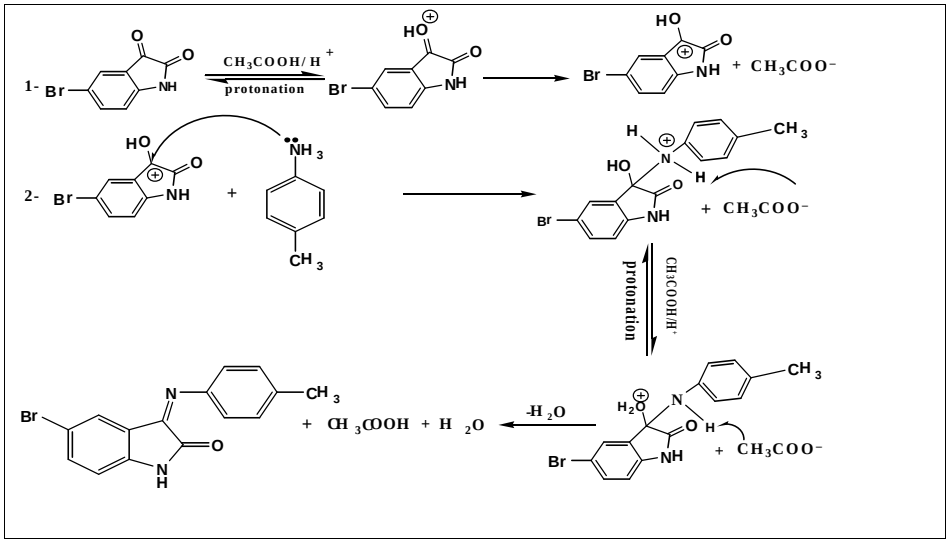

Scheme 2: Mechanism for synthesis of 3-(tolyl-imino)-5-bromo indole-1H-2-one.

Synthesis of N-(α-chloroaceto-1-yl)-3-(*P*-tolyl imino)-5-bromo-2-oxo indole (2)

A mixture of 3-(tolyl imino)-5-bromo indole-1H-2-one compound (1) in dimethylformamide (DMF), and sodium hydride periodically added to the solution in small portions of chloroacetylchloride to give compound (2), Scheme 3 [44].

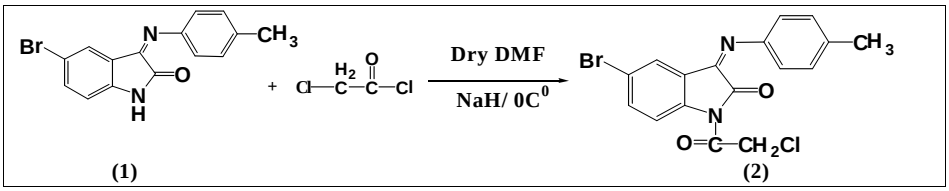

Scheme 3: Synthesis of N-(α-chloroaceto-1-yl)-3-(P-tolyl imino)-5-bromo-2-oxo indole

Compound (2) was synthesized by nucleophilic substitution reaction of compound (1) with Chloroacetylchloride. This reaction was carried out in sodium hydride (NaOH) solution to increase the nucleophilicity of indole in attacking molecule by forming sodium salt as an intermediate [45], Scheme 4.

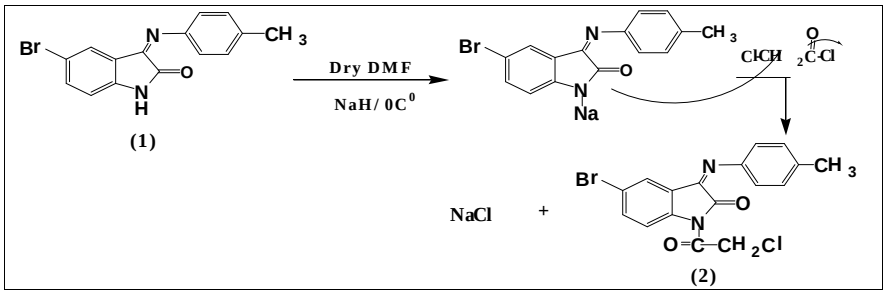

Scheme 4: The forming of sodium salt as an intermediate

Synthesis of N-(acetohydrazide-1-yl)-3-(P-tolyl imino)-5-bromo-2-oxoindole (3)

The N-(acetohydrazide-1-yl)-3-(P-tolyl imino)-5-bromo-2-oxoindole (3) was found a suitable route for this synthetic approach. So when compound (2) refluxed with hydrazine hydrate in dimethylformamide as a solvent it gave the expected compound (3), Scheme 5**.**

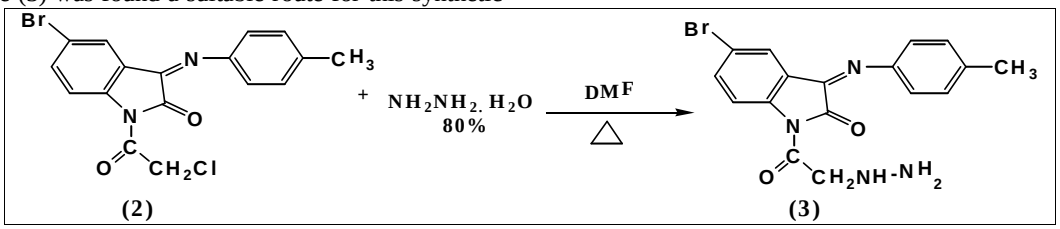

Scheme 5: Synthesis of N-(acetohydrazide-1-yl)-3-(P-tolyl imino)-5-bromo-2-oxoindole.

Synthesis of N-[(6-nitro-1, 2-dihydrophtalazin-3, 10-dione-1-yl) aceto] 3 (tolylimino)-5-bromo-2-oxoindole (4).

This compound was synthesized by the reaction of the N-(acetohydrazide-1-yl)-3-(P-tolylimino)-5-bromo-2oxoindole (3), with (4-nitrophthalic anhydride) in the presence of acetic acid as solvent and catalyst. This compound was summarized in scheme 6. The suggested mechanism for the synthesis of the previous derivative can be explained as the following general mechanism [46], and physical properties of 5BIN (compound (4)) is listed in Table 7. FTIR spectral data of compound (4) and HNMR signals for compound 5BIN (ppm) are listed in Table 8.

TABLE 7: Physical properties of compound 5BIN.

Molecular Formula	M.W g/mol	m.p. ^{o}C	Yield %	Color	Solvent for recryst.
$C_{25}H_{16}BrN_5O_6$	562.3	158-159	85	Deep yellow	Chloroform

TABLE 8: FTIR modes of vibration (cm^{-1}) and HNMR signals (ppm) for compound 5BIN

νN-H	ν(C-H) arom.	ν(C-H) aleph.	νC=O	ν(C=N)	Others
3230	3066 3035	2954 2923	1708 1689	1668	νNO_2 asym. 1515, sym. 1373
HNMR signals					
3.30 (s, 3H, $-CH_3$); 4.30 (s, 2H, $-CH_2$-); 6.85 (s,1H, $-CH_2$-NH-) 7.05-8.35 (m, 10H, Ar-H)					

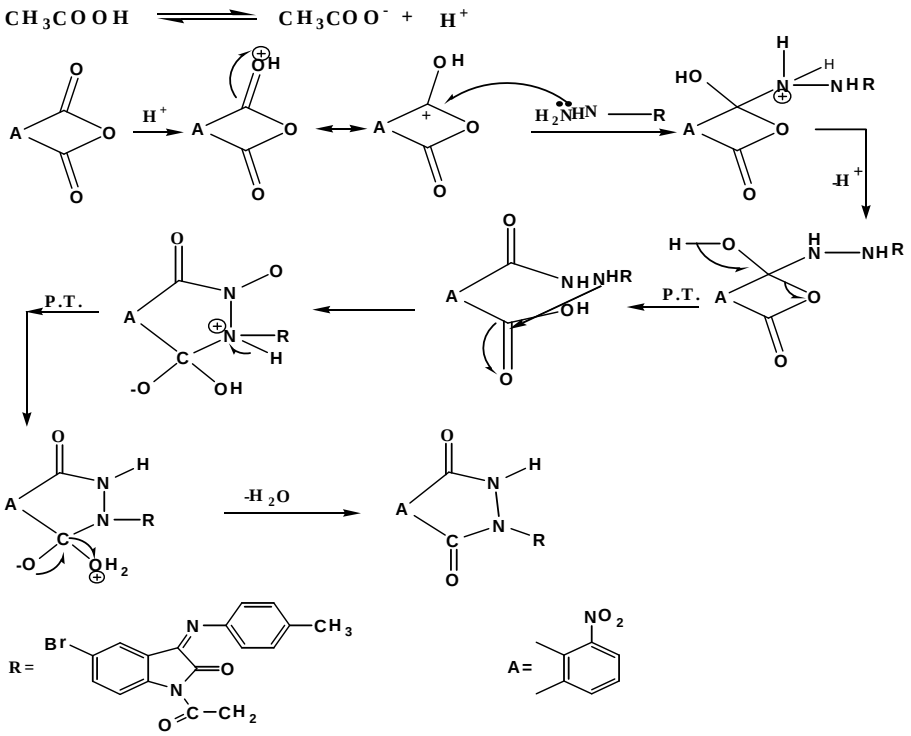

Scheme 6: Mechanical for synthesis of N-[(6-nitro-1,2-dihydrophtalazin-3,10-dione-1-yl) aceto] 3 (tolylimino)-5-bromo-2-oxoindole**.**

Corrosion inhibition process

Inhibitor concentrations.

The inhibition efficiency for each prepared concentration (5, 10, 20, 30ppm) was measured for at temperatures of (293, 303, 313, 323, and 333K). The optimum condition were found to be (5ppm) and (303K). Other concentrations were also measured at the different temperatures for the thermodynamic properties.

Potentiodynamic Polarization Measurements

Potentiodynamic polarization testing of carbon steel C45 in inhibited and uninhibited solution were conducted to measure the corrosion parameters such as corrosion potential E_{corr}, corrosion current I_{corr}, resistance of polarization (R_P) and corrosion rate CR_{corr}. They were studied by recording anodic ba and cathodic bc Tafel slope potentiodynamic polarization curves. Measurements were performed in 3.5% NaCl solution containing different concentrations of the 5BIN inhibitor. The linear Tafel segments of anodic and cathodic curves were extrapolated to corrosion potential to obtain the corrosion current densities I_{corr} and inhibition efficiency percentage IE%, Equation 5:

$$\%IE = \frac{I_{corr(un)} - I_{corr(in)}}{I_{corr(un)}} \times 100 \ldots . (5)$$

Where $I_{corr\ (in)}$ is the inhibited corrosion current densities, $I_{corr\ (un)}$ is the uninhibited current densities. The value of the polarization resistance (Rp) was calculated using Equation 6 [47-50]

$$Rp = \frac{b_a \times b_c}{2.303(b_a + b_c) \times I_{corr}} \quad (6)$$

The surface coverage (Θ) of the corrosion for C.S immersed in 3.5% NaCl solution containing different 5BIN concentration (C) could be estimated, using Equation7.

$$\Theta = \frac{\%IE}{100} \quad (7)$$

The corrosion rate ($CR_{corr.}$) was calculated by Equation 8.

$$CRcorr = I_{corr} \times 0.249 \ldots (8)$$

The addition of the 5BIN derivative causes a decrease in the corrosion rate, i.e. shifts the cathodic and anodic curves to lower values of current densities, and both cathodic and anodic reactions of carbon steel electrode corrosion are inhibited by the 5BIN in 3.5% NaCl. Figure 4 shows Tafel curves anodic and cathodic polarization for the corrosion of carbon steel (C45) in solutions of 3.5% NaCl, with and without the addition of various concentrations of 5BIN at the optimum conditions [5ppm with temperature of 303K]. Table 9 collects the values of $CR_{corr.}$ for C.S surface and inhibition efficiency of the studied compound at various concentrations and different temperature, showing that increasing temperature lead to increase the Icorr, while IE% enhances with the increasing the 5BIN concentration. The optimum conditions for 5BIN were observed at 303K and 5ppm, corresponded to lowest $I_{corr.}$(0.051 µA.cm^{-2}) and maximum IE% (99.96%). The values of iron CR were decreased with increasing concentration of 5BIN and the addition of 5BIN to blank solutions increased the cathodic and anodic current densities without shifting the corrosion potential, so 5BIN can be described as a mixed-type inhibitor. Its inhibition caused by adsorption and the inhibition effect results from the reduction of the reaction area on the surface of the carbon steel [51].

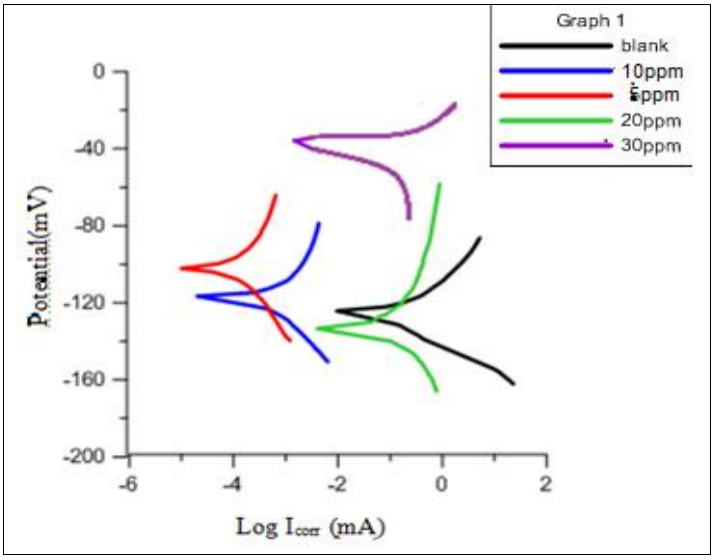

FIGURE 4: Plots of polarization for carbon steel in 3.5% NaCl for blank and for 5BIN inhibitor at a temperature of 303K and various concentrations.

Potentiodynamic polarization curves

The electrochemical corrosion parameters are presented in Table 9 such as corrosion potential (E_{corr}), cathodic and anodic Tafel slopes (bc, ba) and corrosion current density (I_{corr}) obtained by extrapolation of anodic and cathodic regions of the Tafel lines. Figure 5 presents potentiodynamic polarization curves for carbon steel in 3.5% NaCl containing different conditions of 5BIN. However, I_{corr}, E_{corr}, ba and bc were evaluated from the experimental results using a user defined function of ''Non-linear least squares curve fit''. In this calculation, the potential domain is limited to 100 mV/sec of E_{corr}. Table 9, summarizes the obtained corrosion kinetic parameters. E_{corr} and the kinetic parameters calculated by a non-linear regression calculation from the anodic polarization scans near the open circuit potential are found to be similar to those determined from the cathodic polarization scans, and though Icorr is slightly higher. Table 9 also, shows that the $CR_{corr.}$ of carbon steel increases with increasing temperature both in uninhibited and inhibited solution. However, the CRcorr increases more rapidly with temperature in the absence of inhibitor. These results confirm that 5BIN act as an efficient inhibitor in the range of the studied temperature.

TABLE 9: Electrochemical data of the C.S corrosion in 3.5% NaCl at various concentrations of 5BIN and different temperature

Solun.	T (K)	E_{corr} (mV)	I_{corr} ($\mu A.cm^{-2}$)	bc ($mV.dec^{-1}$)	ba ($mV.dec^{-1}$)	IE%	Ɵ	CR
Blank 3.5% NaCl	293	-560.0	89.22	-166.1	92.9	------	------	22.21
	303	-621.0	121.69	-146.9	82.1	------	------	30.30
	313	-785.7	164.53	-26.3	73.8	------	------	40.96
	323	-608.0	191.16	-102.0	315.2	------	------	47.59
	333	-767.2	259.55	-84.5	382.6	------	------	64.62
5ppm	293	-621.0	0.060	-53.5	60.2	99.93	0.999	0.01
	303	-617.3	0.051	-94.9	92.2	99.96	0.999	0.01
	313	-566.6	0.065	-115.7	108.0	99.95	0.999	0.02
	323	-583.5	0.249	-63.9	67.7	99.86	0.998	0.06
	333	-663.9	1.67	-47.6	62.6	99.35	0.993	0.41
10ppm	293	-664.3	0.073	-137.7	137.9	99.91	0.999	0.02
	303	-510.9	0.157	-222.5	289.8	99.87	0.998	0.04
	313	-646	0.158	-97.5	105.6	99.90	0.999	0.04
	323	-704.8	0.210	-114.0	94.8	99.89	0.998	0.05
	333	-714.4	0.329	-105.0	126.3	99.87	0.998	0.08
20ppm	293	-718.2	11.14	-57.8	82.9	87.51	0.875	2.77
	303	-683.8	11.39	-55.3	64.1	90.64	0.906	2.84
	313	-702.2	14.24	-48.4	46.0	91.34	0.913	3.54
	323	-768.1	18.11	-49.6	63.8	90.52	0.905	4.50
	333	-666.7	34.65	-38.0	82.2	86.64	0.866	8.62
30ppm	293	-624.7	1.94	-74.1	73.8	97.82	0.978	0.50
	303	-627.4	2.31	-85.1	103.9	98.10	0.981	0.58
	313	-726.4	3.09	-36.5	26.9	98.12	0.981	0.77
	323	-176.7	3.16	-217.4	33.1	98.34	0.983	0.79
	333	-672.3	6.73	-108.4	110.4	97.40	0.974	1.68

Activation parameters for the corrosion process

In order to evaluate the activation energy of the corrosion process study the temperature can be affected the C.S corrosion in the 3.5% NaCl on the efficiency of inhibition of 5BIN. The effects of temperature were studied in the ranges of 293 to 333K. The values of the corrosion rate in the absence and presence of the optimal concentration of 5BIN at different temperatures are given in Table 10. The reveals data suggests that the $CR_{corr.}$ obtained increases with increasing temperature for the inhibited and uninhibited. This may explain why inhibitory molecules act by adsorption on the metal surface. The activation parameters for the corrosion process were calculated from the equation of Arrhenius (9, 10) are used for the formation of the activation complex in the transition state using transition equations [52]:

$$\log CR = logA - \frac{Ea}{2.303 \times RT} \quad \ldots(9)$$

$$log\frac{CR}{T} = \log\left(\frac{R}{N\square}\right) + \frac{\Delta s*}{2.303} - \frac{\Delta H*}{2.303 \times RT} \ldots..(10)$$

Where, $CR_{corr.}$ is the corrosion rate, A is the pre-exponential constant Arrhenius, Ea is the apparent activation energy of the corrosion, R is the universal gas constant (8.314 $J.mol^{-1}.K^{-1}$), T is the absolute temperature, N is the number of Avogadro constant Planck (6.022 $x10^{23}$ mol^{-1}), h is Plank's constant (6.626 x 10^{-34} J.s), ΔS^* is the entropy of activation and ΔH^* is enthalpy of the activation. This equation can be represented graphically by plotting the natural (log $CR_{corr.}$) versus (1/T) with and without addition of various concentrations of 5BIN in the 3.5% NaCl. The positive values of enthalpy ΔH^* in the absence and presence of various concentration of 5BIN inhibitor Table 10, reflect the endothermic nature of carbon steel activation complex forming, meaning that dissolution of carbon steel is difficult [53]. The value of (Ea) in the presence of 5BIN are higher than that in the uninhibited 3.5% NaCl solution. The lower (A) and higher (Ea) lead to the lower $CR_{corr.}$. The high values of (Ea) in the presence of 5BIN, Table10 can be correlated with the increasing thickness of the double layer that enhances the Ea of the corrosion process [54]. Straight lines were obtained with a slope of (ΔH^*/ 2.303R) and an intercept of [log(R/ Nh)+ (ΔS^*/ 2.303R)] from which the values of $\Delta H^*$and ΔS^* respectively were listed also in Table 10. The positive

values of ΔH^* both in the absence and presence of SEC reflect the endothermic nature of the steel dissolution process. The values of enthalpy of activation ΔH^* were calculated from graphical and mathematical models. The negative values of the entropy of activation both in the absence and presence of 5BIN imply that the activated complex in the rate determining step represents an association rather than a dissociation step.[55,56]. Utilizing the values of ΔH^* and ΔS^*, the values of ΔG^* for the corrosion process could be calculated from the following relation: $\Delta G^* = \Delta H^* - T\Delta S^*$.

TABLE 10: Activation parameters for the C.S dissolution in 3.5% NaCl in the absence and presence the optimum concentration of 5BIN inhibitor

Solun.	T (K)	ΔH^* (kJ.mol^{-1})	ΔG^* (kJ.mol^{-1})	ΔS^* (kJ. mol^{-1}.K^{-1})	Ea (kJ.mol^{-1})	A (Molecules) (cm^{-2}.s^{-1})
Blank 3.5% NaCl	293	18.424	88.451	-0.239	21.020	7.57873E+28
	303		90.841			
	313		93.231			
	323		95.621			
	333		98.011			
5ppm (5BIN)	293	71.040	173.297	-0.349	73.623	4.24225E+34
	303		176.787			
	313		180.277			
	323		183.767			
	333		187.257			

The activation energy (Ea) at the optimum concentration (10 mg/L) of 5BIN was determined by plotting (log CR) versus (1/T) as shown in Figure 5.

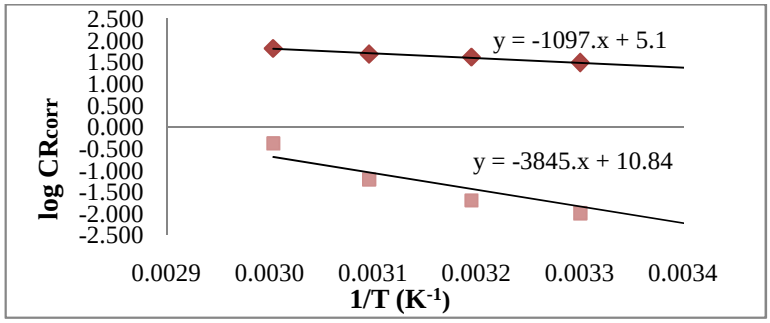

FIGURE 5: Plot of (log $CR_{corr.}$) vs (1/T) for the corrosion of C.S in 3.5% NaCl at the optimum concentration (5mg/ L) of 5BIN within the blank.

The enthalpy of activation ΔH* is obtained from the slope ($-\Delta H^*$/ 2.303 R) obtained by plotting (log $CR_{corr.}$/ T) versus (1/ T) with an intercept of [(log (R/ Nh) +(ΔS^*/ 2.303 R)] Figure 6. The positive value of enthalpy ΔH^* in the absence and presence of various concentration of 5BIN reflects the endothermic nature of carbon steel activation complex forming, meaning that the dissolution of C.S is difficult [53].

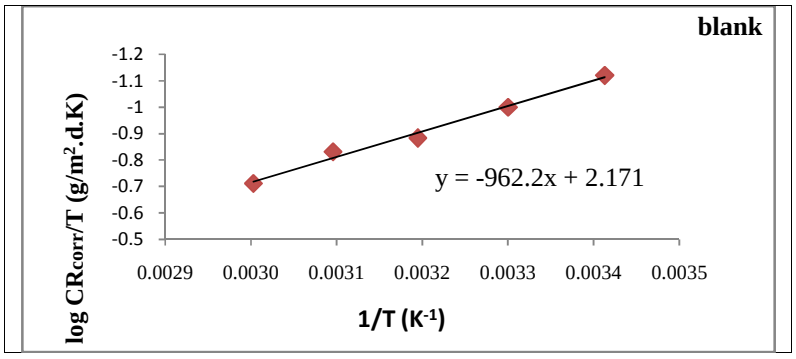

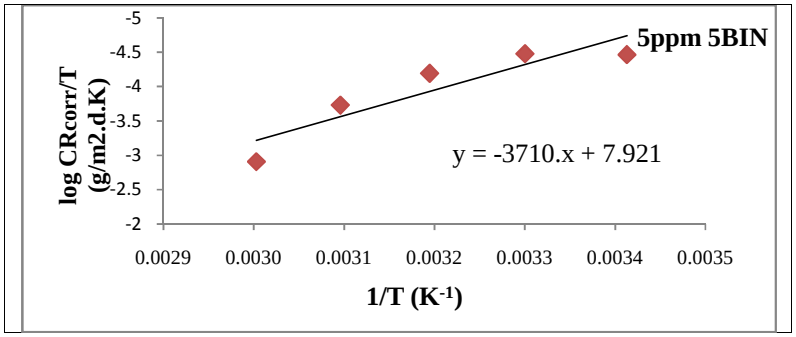

FIGURE 6: Arrhenius plots calculated for CRcorr of C.S in 3.5% NaCl in the absence and presence (5mg/L).of 5BIN.

Adsorption isotherm behavior

The adsorption isotherms are considered to describe the interactions between the 5BIN with the active sites on mild steel. The 5BIN to be a successful corrosion inhibitor depends mainly on the adsorption capacity of the inhibitor on the metal surface [54]. Where (IE%) represent efficiency inhibition percentage measured by the potentiostatic method. Langmuir adsorption isotherm can be represented by the following equations [55].

$C/\Theta = (1/K_{ads}) + C$…. (11)

$C/\Theta = 1/b + C$ (12)

A plot of C/Θ values against the corresponding values of C was found to be linear for the adsorption of 5BIN on carbon steel at different temperatures, Figure 7, and at 303K Figure 8. The term b is the maximum adsorption quantity at different temperature and could be obtained from the intercepts of plotting C/Θ values against concentrations and it could be used to determine the thermodynamic function. For the process of adsorption on C.S surface, these functions are (ΔH_{ads}, ΔS_{ads} and ΔG_{ads}) Table 11, were calculated using equations 13, 14 [56,57].

$$Kads = \frac{1}{55.55} \text{Exp}\left(\frac{-\Delta G}{RT}\right) \quad (13)$$

$$\Delta G_{ads} = -2.303\, RT\, \text{Log}\,(55.55\, K_{ads}) \quad \ldots (14)$$

Whereas, R is the universal gas constant (J. K^{-1}. mol^{-1}), T is the absolute temperature (K), and 55.5 is the molar concentration of water in the solution (mol L^{-1}). By plotting Kads versus (1/T) the ΔG^0_{ads} was extracted from the slope, using equations 15,16.

$$\Delta G^0_{ads} = -RT \ln K_{ads} \ldots \quad .(15)$$

$$\Delta G^0_{ads} = \Delta H^0_{ads} - T\Delta S^0_{ads} \ldots \quad (16)$$

ΔH^0_{ads} and ΔS^0_{ads} are the enthalpy and entropy changes of the adsorption process respectively. A plot of ΔG^0_{ads} versus T was linear with the slope equal to $-\Delta S^0_{ads}$ and intercept of ΔH^0_{ads}, Table 12 collects the Langmuir adsorption parameters for the inhibitors adsorption at the optimum 5BIN concentration. High values of K_{ads} mean better inhibition efficiency of the 5BIN inhibitor, i.e., the strong electrical interaction between the double-layer existing at the phase boundary and the adsorbing 5BIN molecules. The negative value of (ΔG) indicates a spontaneous adsorption of the inhibitors on carbon steel. ΔS^0_{ads} refers to random interaction, whenever they are less random whenever inhibitor best, so 5BIN of a fewer ΔS^0_{ads}. (0.01961 kJ mol^{-1} K^{-1}). The negative values of ΔG^0_{ads} indicate spontaneous adsorption onto the C.S surface [58], and strong interactions between 5BIN molecules and the metal surface [59]. Through (ΔH^0_{ads}) value the nature of the adsorption (chemist or physicist) can be determine. At (ΔH^0_{ads}) equal to (-40 kJ. mol^{-1}) or lower (more negative), the adsorption is chemisorptions and at values of (ΔH^0_{ads}) less negative than (-40 kJ. mol^{-1}), the adsorption is physic-sorption. For 5BIN it is equal to (-8.0418 kJ.mol^{-1}) indicating physic-sorption as a result of sharing or transferring electrons from 5BIN molecule to the metal surface to form a coordinate bond [60]. In all cases, correlation factor R^2 was found to be greater than 0.9880 meaning a reliable result. The adsorption parameters obtained from this studying are listed in Table 11. Figure 9 shows the relationship between log K_{ads} vs (1/T).

TABLE 11: Langmuir adsorption parameters for the 5BIN adsorption at the optimum concentration

T (K)	K_{ads} (L mol^{-1})	ΔG_{ads} (kJ.mol^{-1})	ΔH_{ads} (kJ.mol^{-1})	ΔS_{ads} (kJ.$mol^{-1}K^{-1}$)	R^2
293	10^6×5.02	-13.79	-8.0418	19.6135x10^{-3}	0.9894
303	10^6×4.85	13.99-			0.9946
313	10^6×4.14	14.19-			0.9955
323	10^6×3.98	14.39-			0.9942
333	10^6×3.41	14.59-			0.9881

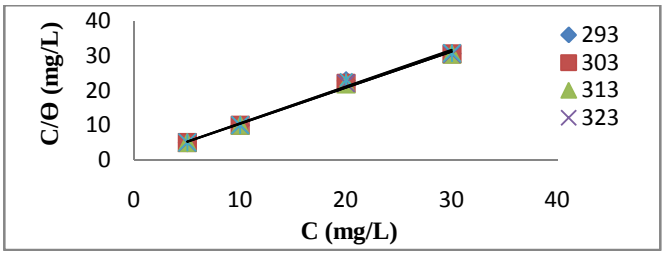

FIGURE 7: Langmuir isotherms plot for the adsorption of 5BIN on carbon steel at different temperatures.

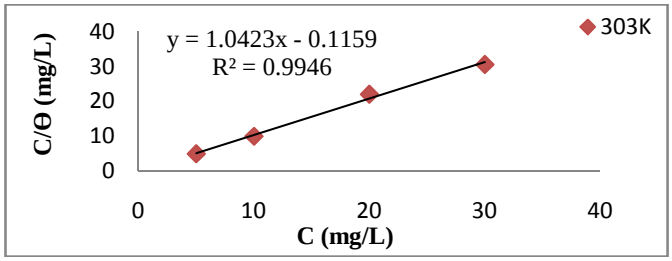

FIGURE 8: Langmuir isotherms plot for the adsorption of 5BIN on carbon steel at 303K.

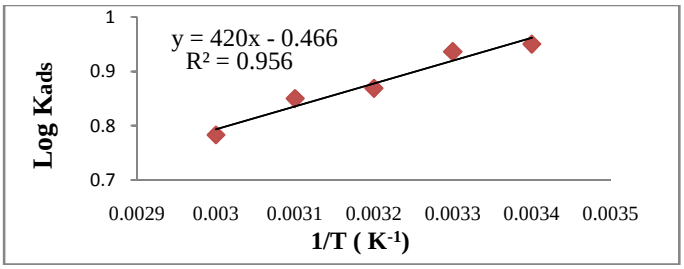

FIGURE 9: Plot of log K_{ads} vs (1/T) for 5BIN inhibitor.

Scanning Electron Microscopy (SEM)

The image SEM for C.S surface with 3.5% NaCl in absence of 5BIN reveals that it consists of spherical particles formed by aggregation, with characteristic uniform corrosion of C.S in 3.5% NaCl solution in the presence of (5 mg/L).of 5BIN, indicated that the composite phase between the C.S surface and the inhibitor was established and the inhibitor 5BIN dispersed on the surface of the C.S base. Considering the inhomogeneous nature of metallic surfaces resulting from the existence of lattice defects and dislocations, a corroding metal surface is generally characterized by multiple adsorption sites having definite activation energies and heat of adsorption. 5BIN inhibitor molecules may thus be adsorbed more readily at surface active sites having suitable adsorption enthalpies, so the SEM image reveals the agglomeration of the inhibitor in some places [61]. The image of SEM in Figure 10 (a, b) shows the particles of 5BIN are likely spherical in nature, uniformly distributed and coverage on carbon steel surface. The scale bar for this image is 100µm and the energy of the acceleration beam employed was 20kV.

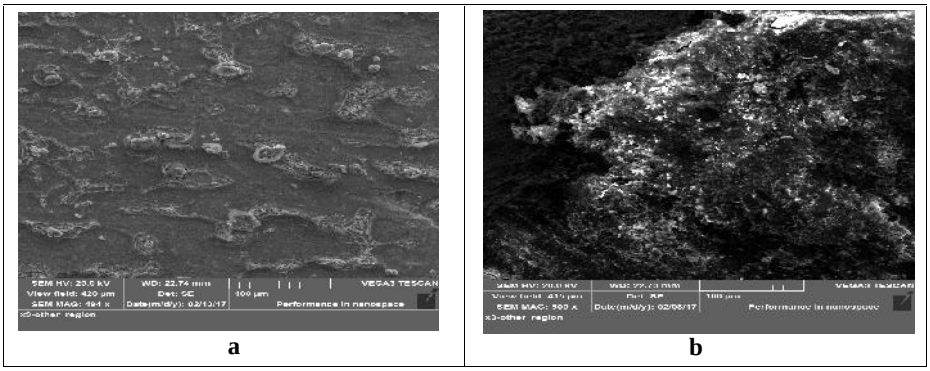

a **b**

FIGURE 10: SEM image of C.S surface with 3.5% NaCl (a) in the absence of (5mg/L).of 5BIN, (b) in the presence of (5mg/L).of 5BIN.

Atomic Force Microscopy (AFM)

The three-dimensional AFM morphologies and cross-sectional profile was measured for carbon steel surface immersed in 3.5% NaCl in the absence and in the presence of 5BIN at the optimum concentration. Peak-to-valley value of AFM image analysis was performed to obtain the average roughness Sa (the average deviation of all points roughness profile from a mean line over the evaluation length), root-mean-square roughness, Sq (the mean measured deviations of height that were taken in the assessmentlength and measurement from the mean line), and peaks of peak-peak Sy height values (greater peak-peak height in five adjoining sampling heights). Figures 11 (a,b,c) display the metal surface is corroded with a few holes or pits in the absence of the 5BIN immersed in 3.5% sodium chloride. The (Sa), (Sq), (Sy) carbon steel surface is 3.97nm, 4.89nm, and 34.3nm, respectively. Figures 11 (d, e, f) display the surface of the steel after immersion in 3.5% NaCl solution in presence of 5BIN. The (Sa), (Sq), (Sy) for carbon steel surface are 0.852nm, 1.2nm, and 25.9nm, respectively. Elevation values (Sa), (Sq), (Sy) height values are lower in the presence of 5BIN inhibitor compared to absence of it, confirm that the surface is smoother. Surface softness is due to the formation of a protective film built-in of the 5BIN on the surface of the metal, there is by inhibiting the corrosion of carbon steel [62].

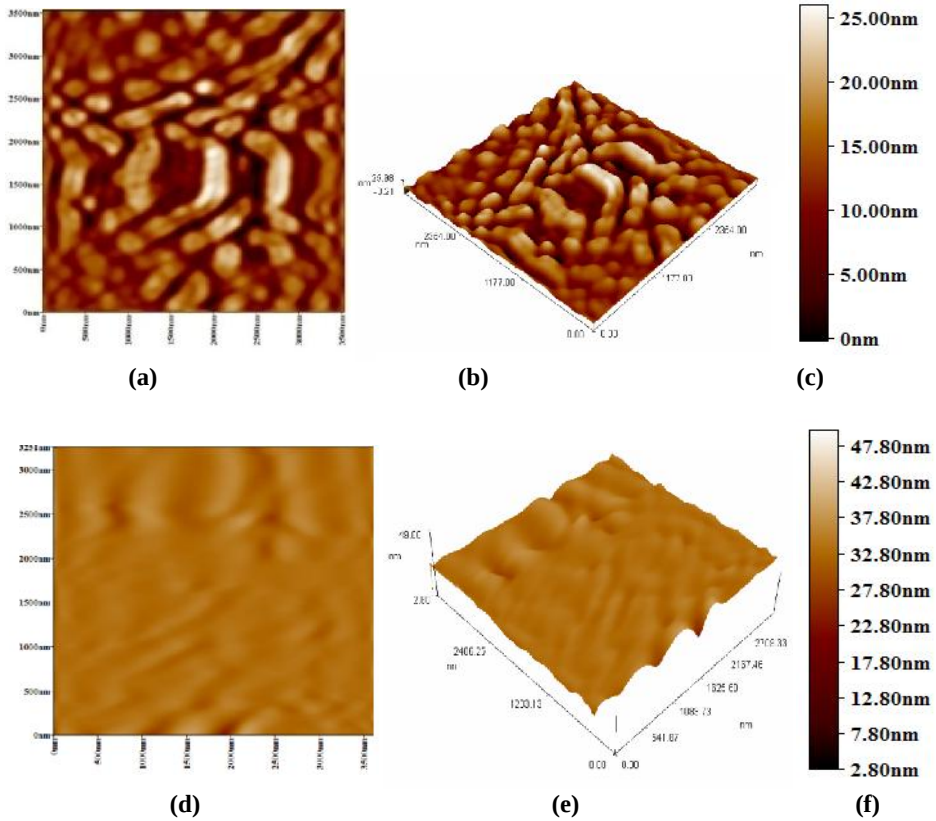

FIGURE 11: AFM images (three dimentional) of the surface of C.S in 3.5% NaCl solution in the absence and presence 5BIN inhibitor.

Energy Dispersive Spectroscopy (EDS**)**

Energy Dispersive Spectroscopy EDS allows one to identify what those particular elements are and their relative proportions atomic%. By scanning the beam in raster and displaying the intensity of a selected X-ray line. Figure 12 (a,b) shows a characteristic spectrum collected by EDS, peak position give the energy of detected X-rays emitted from a sample as it is being bombarded by electrons in the microscope. By comparing the peak energies to the labelated emission energies for all of the elements, the constituent elements of the sample can be identified. Furthermore, by comparing the area under each peak to a set of standards with known elemental concentrations. It has been found that the ratio of the two elements (Fe, O) in 3.5% NaCl in the absence of 5BIN are (68.4, 28.1) wt% more than (32.3, 22.6) wt% in presence of 5BIN inhibitor. These results indicate the formation of a layer of the inhibitor on CS surface for reducing the proportion of the metal (Fe) and oxygen (O).

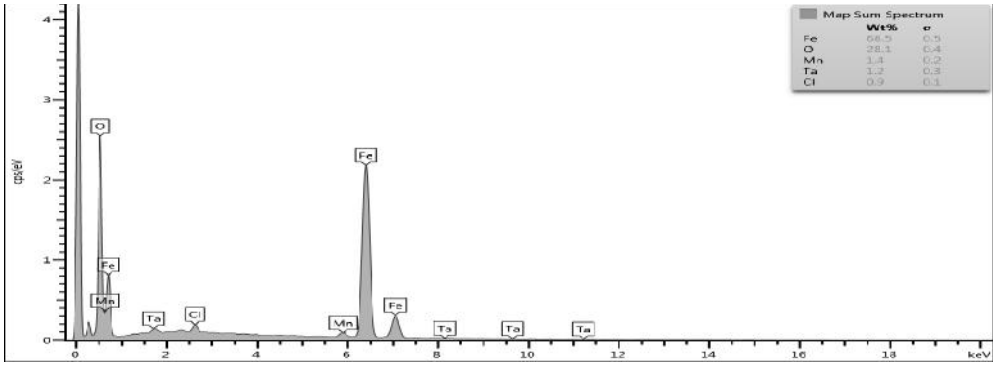

Figure 12a: EDS spectrum of the surface of C.S in 3.5%NaCl solution in the absence of the 5BIN inhibitor.

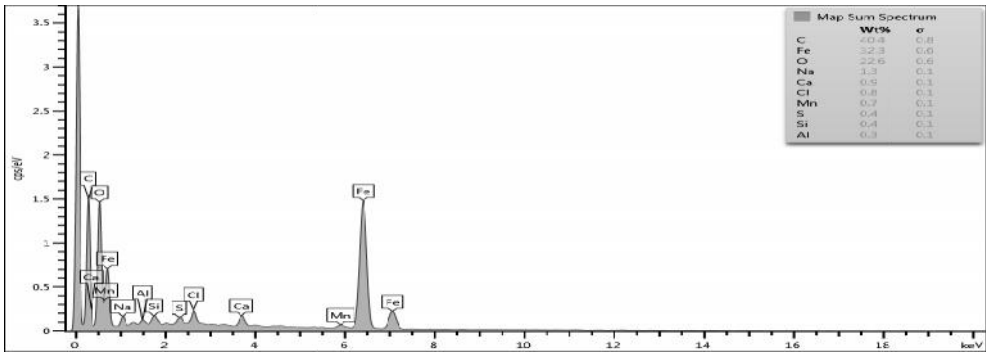

Figure 12b: EDS spectrum of the surface of C.S in 3.5% NaCl solution in presence of the optimum concentration of 5BIN.

Compared to the previous 5-Nitro derivatives that were prepared and studied as theoretical and practical inertia inhibitors, which differ in the offset aggregates, the results obtained show that the current compounds are much better [28,29].

CONCLUSION

The corrosion inhibition of carbon steel in 3.5%.NaCl solution by 5BIN was studied theoretically by using PM3 and DFT quantum mechanical calculations and experimentally by using electrochemical techniques. According to these studies findings, it could be concluded that:

Computational studies is a very important tool to find the most stable inhibitor conformation and adsorption sites for a broad range of materials. This information can help to gain further insight into the corrosion system, such as the most likely point of attack for corrosion on a surface, the most stable site for inhibitor adsorption and adsorption density of the inhibitor for the adsorbed layer.

The local reactivity has been studied through the Mulliken charges population analysis in order to predict both the reactive sites of nucleophilic and electrophilic attacks.

The polarization curves showed that the 5BIN acts as a mixed-type inhibitor.

The adsorption of 5BIN on the steel surface from 3.5%.NaCl solution follows Langmuir adsorption isotherm.

The thermodynamic parameters suggest that this inhibitor could be strongly adsorbed on the carbon steel surface so it is expected to be a very good corrosion inhibitor for the carbon steel protection in 3.5%.NaCl solution.

DFT and electrochemical studies show clearly that there is an adsorption layer formed on the the metallic surface by giving p-electron density from delocalization region through its HOMO orbital to the LUMO metal.

ACKNOWLEDGEMENTS

The authors thank the staff of the laboratory of organic chemistry, college of science, University of Baghdad, to assist in the preparation of organic derivatives, as well as the staff of the laboratories of University of Technology to provide some techniques and measurements required to complete the research

REFERENCES

[1]. Z. Tribak, Y. Kharbach, A. Haoudi, M.K. Skalli, Y. Kandri Rodi, M. El Azzouzi, A. Aouniti, B. Hammouti, O. Senhaji. Study of new 5 Chloro Isatin derivatives as efficient organic inhibitors of corrosion in 1M HCl medium: Electrochemical and SEM studies, J. Mater. Environ. Sci. 7(6), (**2016**) 2006-2020.

[2]. C. Liang, J. Xia, D. Lei, X. Li, Q. Yao and J. Gao. Synthesis, in vitro and in vivo antitumor activity of symmetrical bis-Schiff base derivatives of isatin, Eur J. Med Chem, 74 (**2013**) 742-750.

[3]. A. Zarrouk, B. Hammouti, A. Dafali and F. Bentiss. Inhibitive properties and adsorption of purpald as a corrosion inhibitor for copper in nitric acid medium, industrial and engineering Chemistry. Res. 52(7), (**2013**) 2560-2568.

[4]. H. Elmsellem, A. Aouniti, M. Khoutoul, A. Chetouani, B. Hammouti, N. Benchat, R. Touzani,

and M. Elazzouzi. Theoretical approach to the corrosion inhibition efficiency of some pyrimidine derivatives using DFT method of mild steel in HCl solution**,** J. Chem. Pharm. Res., 5(4), **(2014**) 2016-2024.

[5]. P. Pakravan, S. Kashanian, M.M. Khodaei. and F.J. Harding, Biochemical and pharmacological characterization of isatin and its derivatives: from structure to activity, Pharmacological Reports, 65, (**2013)** 313-335.

[6]. K. Al Maamari. Isatin derivatives: synthesis, reactivity and anti corrosion properties. Ph.D. Thesis. Department of Chemistry, Faculty of Science, University of Mohammed-V-Agdal, Rabat, 25 July **2013**.

[7]. T. Sandmeyer and C. Helv. Synthesis of substituted isatins, Chim. Acta., 2, (**1919**) 232-234.

[8]. M. Ischia, M.A. Palum and G. Prota. Adrenalin oxidation revisited. New products beyond the adrenochrome stage, Tetrahedron. 44, (**1988**) 6441-6446.

[9]. GK. Jnaneshwara, AV. Bedekar and VH. Deshpande. Microwave assisted preparation of isatins and synthesis of (±)-convolutamydine-A, Journal Synthetic Communications. An International Journal for Rapid Communication of Synthetic Organic Chemistry, 29(20), (**1999**) 3627-3633.

[10]. J. Gasparic, T. Vontor, A. Lycka and D. Snobl. Formation of acetals and cleavage of the five-membered ring in the bromination of isatin in alcohols, Cheminform. 55, (**1990**) 2963-2966.

[11]. a- M.D. Francisco and Herbert, New isatin derivatives: Synthesis and reactions, synthetic metals. Journal elsevier 39(2), (**1990**). 195-203. b-K..A. Al Maamar. ISATIN DERIVATIVESi: SYNTHESIS, REACTIVITY AND ANTI CORROSION PROPERTIES. (**2013**) UNIVERSITY OF MOHAMMED-V- AGDAL. Faculty of Science. Rabat

[12]. a- Y. Guo and F. Chen. TLC-UV-spectrophotometric and TLC scanning determination of isatin in leaf of isatis,. Zhongcaoyao. 17, (**1986)** 8-11.

[13]. b- Laurent A. Recherches sur lindigo. Ann. Chim. Phys., 3(3),(**1840**) pp: 393–434.

[14]. A.M. Vijey, G. Shiny and Vb. Vaidhyalingam synthesis and antimicrobial activities of 1-(5-substituted-2-oxo indolin-3-ylidene)-4-(substituted pyridin-2-yl) thiosemicarbazide, ARKIVOC, 11, (**2008**) 187-194.

[15]. V. RAJ. Review on CNS activity of isatin derivatives, International Journal of Current Pharmaceutical Research . 4(4), (**2012**) 1-9.

[16]. M.A. Amin, S.S.A.E. Rehim and H.T.M. Abdel-Fatah. Electrochemical frequency modulation and inductively coupled plasma atomic emission spectroscopy methods for monitoring corrosion rates and inhibition of low alloy steel corrosion in HCl solutions and a test for validity of the Tafel extrapolation method, Corros. Sci., 51, (**2009**) 882–894.

[17]. F.S. De Souza and A. Spinelli. Caffeic acid as a green corrosion inhibitor for mild steel, Corros. Sci., 51, (**2009**) 642–649.

[18]. H.J. Ahmed Synthesis, characterization and study of antimicrobial activity of some new Schiff base derivatives containing 5-bromo isatin moiety. M.Sc. Thesis. Department of Chemistry, College of Science, University of Baghdad. Baghdad, Iraq. **2015**.

[19]. A.D. Becke. Density-functional thermochemistry. III. The role of exact exchange, J. Chem. Phys., 98(**1993**) 5648-5652.

[20]. C. Ee, W. Yang and R.G. Parr. Development of the Colle-Salvetti correlation-energy formula into a functional of the electron density, Phys. Rev., B41 (**1988**) 785-789.

[21]. R.G. Parr and W. Yang. Density functional approach to the frontier-electron theory of chemical reactivity, Chem. Phys., 106, (**1984**) 4049–4050.

[22]. M.J. Frisch, G.W. Trucks, H.B. Schlegel, G.E. Scuseria, M.A. Robb, J.R. Cheeseman, J.A. Montgomery, J.A. Jr., Vreven, T. Kudin, K.N. Burant, J.C. Millam, J.M. Iyengar, S.S. Tomasi, J. Barone, V. Mennucci, B. Cossi, M. Scalmani, G. Rega, N. Petersson, G.A. Nakatsuji, H. Hada, M. Ehara, M. Toyota, K. Fukuda, R. Hasegawa, J. Ishida, M. Nakajima, T. Honda, Y. Kitao, O. Nakai, H. Klene, M. Li, X. Knox, J.E. Hratchian, H.P. Cross, J.B. Bakken, V. Adamo, C. Jaramillo,J. Gomperts, R. Stratmann,R. E. Yazyev, O.Austin, A.J. Cammi,R. Pomelli,C Ochterski, J.W. Ayala, P.Y. Morokuma, K. Voth, G.A. Salvador, P. Dannenberg, J.J. Zakrzewski, V.G. Dapprich, S. Daniels, A.D. Strain, M.C. Farkas, O. Malick, D.K. Rabuck, A. D. Raghavachari, K Foresman, J. B. Ortiz,J. V Cui, Q. Baboul, A. G. Clifford, S. Cioslowski, J. Stefanov, B.B. Liu, G. Liashenko, A. Piskorz, P. Komaromi, I. Martin, R.L. Fox, D.J. Keith, T. Al-Laham, M.A. Peng, C.Y. Nanayakkara, A. Challacombe, M. Gill, P.M. W. Johnson B. Chen, W. Wong, M.W. Gonzalez, C. and Pople, J.A. 2009. Gaussian 03, Gaussian. Inc. Pittsburgh PA.

[23]. S.M.H.Al-Majidi and K.T.A.Al-Sultani ,.Al-Mustansiriya, J. Scie. 21(4) (**2010**) 61-72.

[24]. S.M.H Al-Majidi, M. Rafat. and A. Karim. Synthesis and characterization of novel 1,8-Naphthalimide derivatives containing 1,3-oxazoles, 1,3-thiazoles, 1,2,4-triazoles as antimicrobial agents, J. Al-Nahrain University, 16(4), (**2013**) 55-66.

[25]. S.M.H. Al-Majidi and W.W.N.Al-Kaisy, Proceeding of 3rd scientific conference, (**2009**), 1413-1423.

[26]. I.B. Obot and N.O. Obi-Egbedi. 2,3-Diphenylbenzoquinoxaline: A new corrosion inhibitor for mild steel in sulphuric acid, Corros. Sci., 52(1), (**2010**) 282-285.

[27]. S.A. Umoren, I.B. Obot, E.E. Ebenso and N.O. Obi-Egbedi. Synergistic inhibition between naturally occurring exudate gum and halide ions on the

corrosion of mild steel in acidic medium, Int. J. Electrochem. Sci., 3(**2008**) 1029-1043.

[28]. J.O.M. Bockris, M.A. Genshaw, V. Brusic and H. Wroblowa. The mechanism of the passivation of iron. and coulometric investigation, Electrochim. Acta., 16 (**1971**) 1859-1894.

[29]. R.M. Kubba and M.M. Khathem. Theoretical studies of corrosion inhibition efficiency of two new N-phenyl-ethylidene-5-bromo isatin derivatives. Iraqi Journal of Science. 57(2B), (**2016**) 1041-1051.

[30]. R.M. Kubba and M.M. Khathem. PM3 and DFT quantum mechanical calculations of two new N-benzyl-5-bromo isatin derivatives as corrosion inhibitors. Iraqi Journal of Science, 5(8), (**2016**) 16-26.

[31]. R.M. Kubba and A.S. Alag. Experimental and theoretical evaluation of new quinazolinone derivative as organic corrosion inhibitor for carbon steel in 1M HCl solution. International Journal of Science and Research (IJSR) (6), (**2017**) 1832-1643.

[32]. R.M. Issa, M.K. Awad and F.M. Atlam. Quantum chemical studies on the inhibition of corrosion of copper surface by substituted uracils, Appl. Surf. Sci., 255(5),(**2008**).

[33]. M.J.S. Dewar and W. Thiel, Ground states of molecules. 38. The MNDO method. Approximations and parameters, J. Am. Chem. Soc., 99 (1977) 4899-4907.

[34]. R.G. Pearson. Absolute electronegativity and hardness: application to inorganic chemistry, J. Inorganic Chemistry, 27 (**1988**) 734-740.

[35]. J. H. Henriquez-Román, M. Sancy, M. A. Páez, L. Padilla-Campos, J. H. Zagal, C. M. Rangel and G. E. Thompson. The influence of aniline and its derivatives on the corrosion behaviour of copper in acid solution, Journal of Solid State Electrochemistry, 9(7), (**2005**) 504-511.

[36]. V.S. Sastri and J.R. Perumareddi. Molecular orbital theoretical studies of some organic corrosion inhibitors, CORROSION, 53 (**1997**) 617-622.

[37]. I. Lukovits, E. Kalman and F. Zucchi. Corrosion inhibitors correlation between electronic structure and efficiency, CORROSION, 57(1), (**2001**) 3-8.

[38]. H. Chermette. Chemical reactivity indexes in density functional theory, J. Comput. Chem., 20, (**1999**) 129-154.

[39]. P. Zhao, Q. Liang and Y. Li. Electrochemical, SEM/ EDS and quantum chemical study of phthalocyanines as corrosion inhibitors for mild steel in 1 mol/l HCl, Applied Surface Science. 252(5), (**2005**) 1596-1607.

[40]. A. Popova, M. Christov and T. Deligeorigiev. Influence of the molecular structure on the inhibitor properties of benzimidazole derivatives on mild steel corrosion in 1M hydrochloric acid, Corrosion, 59, (**2003)** 756–764.

[41]. R.M. Kubba and F.K. Abood. Quantum chemical investigation of some Schiff bases as corrosion inhibitors for mild steel in hydrochloric acid solutions, Iraqi Journal of Science, 56(2B), (**2015**) 1241-1257.

[42]. A. Stoyanova, G. Petkova and S.D. Peyerimhoff, Correlation between the molecular structure and the corrosion inhibiting effect of some pyrophtalone compounds, Chem. Phys., 279, (**2002**) 1-6.

[43]. X. Li, S. Deng, H. Fu and T. Li. Adsorption and inhibition effect of 6-benzyl aminopurine on cold rolled steel in 1.0 M HCl, Electrochimica Acta., 54(16), (**2009**) 4089-4098.

[44]. M. Herbert, S. Jacob, N. Howard and J. George, "Organic chemistry Schaum's outlines", 4th edition, Mc Graw-Hill Companies, Inc. USA, **2010** .

[45]. N.S. Isaacs. Synthetic routes to β lactams. Chem. Soc. Rev., 5 (**1976**) 181-202.

[46]. J. March. "Advanced Organic Chemistry" 3rd edition, Wiley, New York, USA, **1985**.

[47]. A.I. Vogel, (Textbook of practical organic chemistry) 5th Edition, Longman,**1996**.

[48]. E.S.M. Sherif, R.M. Erasmus and J.D. Comins. In situ Raman spectroscopy and electrochemical techniques for studying corrosion and corrosion inhibition of iron in sodium chloride solutions, Electrochim. Acta 55 (**2010**) 3657–3663.

[49]. E.S.M. Sherif. Effects of 5-(3-aminophenyl)-tetrazole on the inhibition of unalloyed iron corrosion in aerated 3.5% sodium chloride solutions as a corrosion inhibitor, Mater. Chem. Phys., 129 (**2011**) 961–967.

[50]. E.S.M. Sherif, R.M. Erasmus, J.D. Comins. Inhibition of copper corrosion in acidic chloride pickling solutions by 5-(3-aminophenyl)-tetrazole as a corrosion inhibitor, Corros. Sci., 50, (**2008**) 3439–3445.

[51]. M. Es-Saheb, E.S.M. Sherif, A. El-Zatahry, M.M. El Rayes. and A.K. Khalil. Corrosion passivation in aerated 3.5% NaCl solutions of brass by nanofiber coatings of polyvinyl chloride and polystyrene, Int. J. Electrochem. Sci., 7 (**2012**) 10442–10455.

[52]. S. Hong, W. Chen, H.Q. Luo and N.B. Li. Inhibition effect of 4-amino-antipyrine on the corrosion of copper in 3 wt.% NaCl solution, Corrosion Science, 57 (**2012**) 270–278.

[53]. E.E. Ebenso, and I.B. Obot. Inhibitive properties, thermodynamic characterization and quantum chemical studies of secnidazole on mild steel corrosion in acidic medium, Int. J. Electrochem Sci., 5 (**2010**) 2012-2035.

[54]. S.A. Umoren, and I.B. Obot. Polyvinyl pyrollidone and polyacryl amide as corrosion inhibitors for mild steel in acidic medium, Surf. Rev. Lett., 15(3) (**2008**) 277-286.

[55]. M. Tourabi, K. Nohair, A. Nyassi, B. Hammouti, C. Jama, F. Bentiss and J. Mater. Thermodynamic characterization of metal dissolution and inhibitor adsorption processes in mild steel / 3,5-bis(3,4-dimethoxyphenyl)-4-amino-1,2,4-triazole / hydrochloric acid system, J. Mater. Environ. Sci. 5(4) (2014) 1133-1143.

[56]. E.E. Oguzie, V.O. Njoku, C.K. Enenebeaku, C.O. Akalezi and C. Obi. Corros. Effect of

hexamethylpararosaniline chloride (crystal violet) on mild steel corrosion in acidic media, Corrosion Science. 50, (**2008**) 3480-3486.

[57]. C. Chem and X. Wang. Adsorption of Ni(II) from aqueous solution using oxidized multiwall carbon nanotubes, Ind. Eng. Chem. res., 45 (**2000**) 9144-9149.

[58]. S. Karaca, A. Gures, M. Acikyildiz and M. Ejder. Adsorption of cationic dys from aqueous solution by activated carbon, Microporus Mesoporous Mater., 115 (**2008)** 376-382 .

[59]. M. Yadav, S. Kumar and D. Behera. Inhibition effect of substituted thiadiazoles on corrosion activity of N80 steel in HCl solution, Journal of Metallurgy, (**2013**) 1-14.

[60]. A.A. Ghani1, H. Bahron1, M.K. Harun1 and K. Kassim. Schiff bases derived from isatin as mild steel corrosion inhibitors in 1M HCl, The Malaysian Journal of Analytical Sciences. 18(3), (**2014**) 507-513.

[61]. Z. Tribak1, Y. Kharbach1, A. Haoudi1, M.K. Skalli1, R. Kandri Y., M.El. Azzouzi, A. Aouniti, B. Hammouti and O. Senhaji. Study of new 5-Chloro-Isatin derivatives as efficient organic inhibitors of corrosion in 1M HCl medium: Electrochemical and SEM studies. J. Mater Environ. Sci., 7(6), (**2016**) 2006-2020.

[62]. A. Mohamed, K. Abbas, A. Zakaria, O.M. Hamdy, E. Abo and E. Olfat. Synthesis of novel Schiff base silicon compound for employing as corrosion inhibitor for carbon steel in the 1 M HCL and 3.5% NaCl aqueous media, International Journal of Chemical, 3 (**2015**) 2320–4087.

[63]. B.S. Devi and S. Rajendran. Influence of garlic extract on the inhibition efficiency of tri sodium citrate. International Journal of Chemical Science and Technology, 1(**2011**) 79–87.